Cortical hemodynamic response associated with spatial coding: A near-infrared spectroscopy study

Abiot Y. Derbie[1,2], Bolton Chau [1], Bess Lam [1], Yun-hua Fang[3], Kin-Hung Ting[4], Clive Y. H. Wong[1,5], Jing Tao[3], Li-dian Chen[3], Chetwyn C. H. Chan[1,4]

[1]Applied Cognitive Neuroscience Laboratory, Department of Rehabilitation Sciences, The Hong Kong Polytechnic University, Hong Kong

[2]Department of Psychology, Bahir Dar University, Bahir Dar, Ethiopia

[3]College of Rehabilitation Medicine, Fujian University of Traditional Chinese Medicine, Fuzhou, China

[4]University Research Facility in Behavioral and Systems Neuroscience, The Hong Kong Polytechnic University, Hong Kong

[5]Department of Psychology, The University of Hong Kong, Hong Kong

Correspondent Author: Chetwyn C. H. Chan, PhD, Chair Professor, Applied Cognitive, Neuroscience Laboratory, Department of Rehabilitation Sciences, The Hong Kong, Polytechnic University, Hong Kong, CHINA, Tel: 852-2766-6727, E-mail: Chetwyn.Chan@polyu.edu.hk

---

Abstract

Allocentric and egocentric are two different types of spatial coding. Previous studies reported the involvement of the dorsal attention network in both types. To eliminate the possible task-specific confounds in the results, this study employed common tasks to readdress the uniqueness of allocentric (aSC) and egocentric (eSC) spatial coding. Twenty-two participants completed a custom-designed visuospatial task and changes in concentration of oxygenated hemoglobin (O_2-Hb) were recorded using functional near-infrared spectroscopy (fNIRS). The least absolute shrinkage and selection operator-regularized principal component (LASSO-PCR) algorithm was used to identify the cortical sites that predicted the reaction times of the aSC and eSC conditions. Significant changes in O_2-Hb concentration in the right superior frontal gyrus (SFG) and post-central gyrus (PoG) were common to both conditions. In contrast, the changes in O_2-Hb concentration unique to aSC were in the left pre-central gyrus (PG) and intraparietal sulcus (IPS), while that unique to eSC was in the right posterior inferior parietal lobule (IPL). The fNIRS results suggest top-down attention, encoding visual representation, and response-mapping processes were common to both types of spatial coding. When compared with egocentric, allocentric spatial coding tends to demand more orienting attention and updating of spatial information. Future study is to use other visuospatial tasks for further informing the task-specificity in spatial coding processes.

Keywords: fNIRS; IPL; SFG; attention; allocentric spatial coding; egocentric spatial coding

1. Introduction

Decoding visual information for processing involves orienting of attention on the object in space (Chun, Golomb, & Turk-Browne, 2011; Desimone & Duncan, 1995). To respond to a simple question—"Where are you?" for example—an individual would need to make reference to an object in space and indicate his or her position, such as by saying, "I am to your right" or, "I am between two bookshelves." The former is egocentric spatial coding (eSC), in which one's brain encodes an object in space relative to his or her bodily coordinates, whereas the latter is allocentric spatial coding (aSC), in which the brain encodes an object in space with reference to the coordinates of another object in space (Ekstrom, Arnold, & Iaria, 2014; Filimon, 2015). A review of brain imaging literature suggests three different views on the neural processes involved in the two types of spatial coding.

The first view stipulates that the cognitive processes underlying these two spatial coding types are differently subserved by the dorsal and ventral attention networks (Chen, Weidner, Weiss, Marshall, & Fink, 2012; Fox, Corbetta, Snyder, Vincent, & Raichle, 2006; Vossel, Geng, & Fink, 2014). The ventral stream to be predominantly involved in aSC while the dorsal stream involved in eSC (Burgess, 2006; Milner & Goodale, 2008). The second view is that both spatial coding types are mediated by the same group of neural substrates. For instance, the posterior parietal cortex (PPC)(Castiello, 2005; Culham & Valyear, 2006), and the posterior cingulate cortex and the precuneus (Burgess, 2008; Epstein, 2008; Iaria, Chen, Guariglia, Ptito, & Petrides, 2007). The third view is that the neural substrates mediating aSC subsume those mediating eSC (Zaehle et al., 2007). When compared with eSC, aSC involves more of visual working memory (Cooper & Humphreys, 2000) and cognitive resources (for critical review: Ekstrom et al., 2014; Filimon, 2015). The parietal cortex particularly the precuneus as part of the dorsal attention network have been found to mediate these additional neural processes (Ekstrom et al., 2014; Zaehle et al., 2007; Zhang & Ekstrom, 2013).

A review of the studies underpinning each of the three views indicated that, instead of the intrinsic diversities in the neural processes, the contradictory results might have been contributed by the task-taking processes involved in the different behavioral paradigms employed in these studies. With the potential task-specific influences in mind,

among the three views, a recent study conducted by Szczepanski, Pinsk, Douglas, Kastner, and Saalmann (2013) offers further evidence to support the third view, i.e. aSC processes subsume the eSC processes. The findings were that the supplementary eye field (SEF) to the superior parietal lobule (SPL) pathway was common to both conditions; whereas the frontal eye fields (FEF) to the intraparietal sulcus area two and the SEF were unique to the egocentric and allocentric conditions, respectively (Szczepanski et al., 2013). In their study, they employed a cue-to-target paradigm that was different from the overt orienting tasks used in the majority of the previous studies in this area. The advantage of a cue-to-target paradigm is in its covert instead of overt orienting attention which would have largely reduced the biases due to the in-task saccade movements (Posner, 1980). Saccade movements have been found to elicit activities in the FEF and PPC (Dean & Platt, 2006; Zaehle et al., 2007).

The motivation behind this study is that in the task used in Szczepanski et al. (2013) study, the task-taking processes could have been biased the results. The participants were instructed to stare at the fixation cross, which appeared in the middle of the screen, before the cues and the targets appeared. The emphasis on the fixation cross as a reference location could have over-emphasized the gaze-centered process (or called viewer-centered process) in both the spatial coding conditions. As a result, it could have artificially inflated the egocentric processes during the allocentric condition. In this study, we targeted to design task to minimize the drawback mentioned above. In brief, the participate was to attend to the fixation cross before the cue or target appeared. Second, the participants were to engage in fine-grain visual scan and discrimination instead of simple spatial judging in both the eSC and aSC conditions. In contrast to previous neuroimaging studies, which employed fMRI, this study used functional near-infrared spectroscopy (fNIRS) for capturing brain activity during participants' task performance for the following reasons. First, the tasks used to elicit the spatial coding processes were relatively complex, and the operation of fNIRS would offer more flexibility than fMRI in the task-taking environment arrangements. Second, fNIRS is less stringent than fMRI on the control of head movements and body posture during the task performance (Heinzel et al., 2013). We hypothesized that the neural substrates corresponding to the dorsal attention network, which contains the juncture of the precentral and superior frontal sulcus, would be common to both aSC and

eSC conditions. The eCS condition would involve the SPL as compared to the aCS condition would involve the inferior parietal lobule (IPL).

2. Method

2.1 Participants

Through convenience sampling, we recruited 22 university students with a mean age of 26.9 years (*SD* = 4.5). All participants gave informed consent according to the guidelines set by the Human Subjects Ethics Subcommittee. The exclusion criteria included having a history of epilepsy and/or other psychiatric disorders and being left-handed. All participants were right-handed. We explained the purpose and procedure of the experiment to the participants, and we obtained ethical approval for the experiment from the Human Subjects Ethics Subcommittee of the institution where we conducted the experiment.

2.2 The Paradigm

The task design made reference to those of Barrett, Bradshaw, Rose, Everatt, and Simpson (2001) and Au (2014). One trial has five screens arranged in sequence (see Figure 1). First, a blank screen appeared for a variable time of 500 to1000 ms, and we set the mean duration to 600 ms. A 500-ms fixation cross (+) followed the blank screen. The third screen presented a 200-ms in the form of a group of three circles (called the triad). In the triad, one circle was illuminated to indicate the probable location (for eSC) or position (for aSC) of the upcoming target. After the cue, another 500-ms fixation cross reappeared. The 1500-ms target stimulus was in the form of the same triad in which each circle contains a "T" oriented in different directions. Only the circle containing a side-lying "T" was the target circle. The participants were to respond by pressing the "Z" or "M" key on a keyboard. There were valid and invalid trials in each condition. For aSC, a valid trial referred to the target circle occupied the same relative position as the cue. For eSC, a valid trial referred to the target circle occupied the absolute location of the cue. Block design was used to organize the trials. All trials were counterbalanced in terms of the hemi-field distributions, and valid and invalid responses.

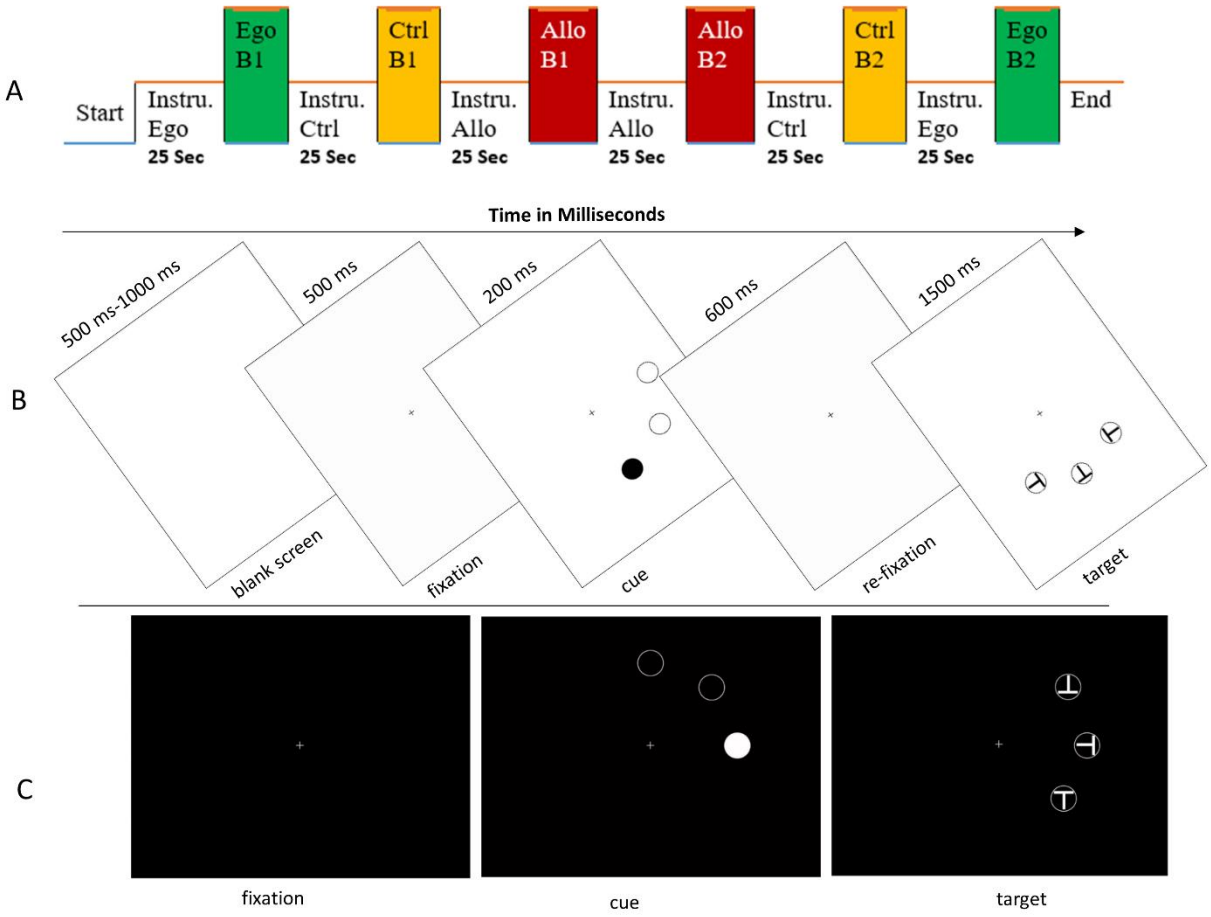

Figure 1. Design of the experimental task. A: Sequence of the six task blocks for the three conditions. B: Presentation schedule of fixing, cue, and target screens of a trial in the egocentric condition. C: Cue and target in a valid trial for the egocentric condition. *Note:* Ego = Egocentric; Allo = Allocentric; Ctrl = Control; B1 = Block 1; B2 = Block 2; Instru = Instruction.

2.2.1 Stimuli

The cue triad stimulus contains three circles appeared on a black background. One illuminated circle indicates the probable location or position of the upcoming target, and the other two circles are the distractors. A total of 22 cue circles appears at different degrees with reference to the middle of the screen (0°, 45°, 90°, 135°, 180°, 225°, 270°, and 315°), equally distributed in the right and left hemi-fields. The target triad stimulus contains one target and two distractor circles (Figure 1B). Target circle is denoted by a 90° or -90° slanted "T," while distractor circle is denoted by "Ts" at a upright or an inverted

orientation. Target and distractor circles are presented in a systematically varied order. The stimuli for the control condition are the same as the cue and target stimuli appeared in the eSC and aSC conditions. The only difference was that the participants were to instruct to view the cue stimulus but to disregard the location/position information contained in it.

2.2.2 Task-taking Procedure

The participants were to complete six task blocks with two blocks for each of the aSC, eSC and control conditions. Each block had 24 trials. The order of the blocks was counterbalanced (Figure 1A). Each participant received training on performing the task before engaging in the experiment. The training continued until the participant responded according to the response rules within 1500 ms in all three conditions. Before commencing the task, the participant sat in front of the computer screen in which the subjective midline of his/her body aligned with the center of the screen. The participant viewed the instructions on the specific response rules at the beginning of the task block. By the end of every trial, the participant responded within 1500 ms by pressing the "M" (90° tilted "T") or "Z" key (-90° tilted "T") to indicate the specific orientation of the target circle. The participant was reminded throughout the task to respond as quickly as possible. We used the E-prime 2.0 software (Psychology Software Tools, Pennsylvania, USA) for Windows 7 with a refresh rate of 56.9 ms for stimulus presentation and behavioral data management.

2.3 NIRS Data Acquisition and Preprocessing

Data capturing of O_2-Hb concentration employed a 52-channel configured Hitachi optical topography (ETG-4000, Hitachi™ Medical. Co., Kashiwa, Japan) equipped with laser diodes of two wavelengths (695 nm and 830 nm). There were 44 channels (22 channels in each hemisphere was composed of two 3 x 5 optode probe sets which each comprising of eight emitters and seven detectors. The data sampling rate was at 10 Hz. The right fNIRS probe was mounted over the right superior frontal region covering the hot sites reported in previous studies on both aSC and eCS. They included the occipitoparietal circuit (e.g. Ekstrom et al., 2014; Filimon, 2015; Galati, Committeri, Sanes, & Pizzamiglio, 2001; Galati et al., 2000; Liu, Li, Su, & Chen, 2017; Neggers, Van der Lubbe, Ramsey, & Postma, 2006) and the right SFG (e.g. Committeri et al., 2004; Fink et al., 2003) (Figure 2). The left probe was

mounted over at 3 cm posterior to the left occipital lobe covering the left temporoparietal junctions and left occipitoparietal circuits. Previous studies revealed that these sites were found to modulate allocentric spatial coding than those in the right superior frontal region (e.g. Chen et al., 2012; Gomez, Cerles, Rousset, Remy, & Baciu, 2014; Saj et al., 2014). The distance between the corresponding source and the detector was 3 cm for detecting the the O_2-Hb concentration at 2–3 cm distance below the scalp (Toronov et al., 2001).

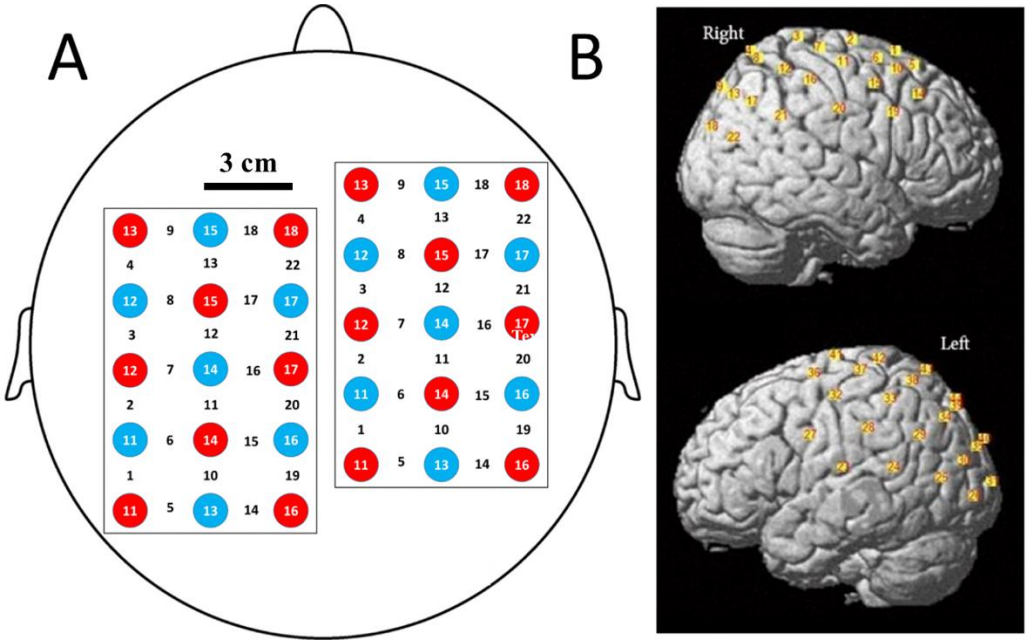

Figure 2. A: Probe set configuration. Red circles represent emitters and blue circles represent detectors. B: Channel configurations superimpose onto T1 image (Montreal Neurological Institute space).

Participant-specific NIRS channel positions were obtained with a 3D digitizer before transformation them into Montreal Neurological Institute (MNI) space equipped in the SPM-NIRS toolbox. Estimation of changes in O_2-Hb level was computed with the modified Beer-Lambert law approach (Cope & Delpy, 1988):

$$A = In\frac{I_{inc}}{I_{det}} = L\mu_a + G$$

whereby Lg (l_0/l): light extinction; I_{inc}: incident light intensity; I_{det}: light intensity as detected; L: path length,; $L\mu_a$: tissue absorption coefficient; and G: signal loss due to light scattering (Kocsis, Herman, & Eke, 2006).

2.3.1 Individual and Group Spatial Analysis

Individual level spatial analysis was conducted using the *nfri_mni_estimation* function (Singh, Okamoto, Dan, Jurcak, & Dan, 2005). The NIRS probe positions were "probabilistically" converted into the MNI-152-compatible canonical brain map for deriving the mean cortical surface MNI coordinates for each participant. The individual functional data were entered into the aSC > control and eSC > control comparisons. The *t* values of each contrast for each channel were extracted and then pooled to form the group values. The group mean *t* values for each channel were converted into the functional data and plotted onto the MNI template (Figure 5). The SPM Anatomy Toolbox (Eickhoff et al., 2005) in the SPM5 software package (www.fil.ion.ucl.ac.uk/spm/software/spm5/) was used for producing the anatomical labeling. All operations were conducted in the Matlab environment R2009b (Mathworks, Boston, MA, USA).

2.4 Statistical Analysis

The between-condition reaction times (RTs) of participants obtained from the experimental task were compared with repeated measures analysis of variance. The Validity × Condition effects were tested of which Validity was valid versus invalid trials, and Condition was aSC versus eSC. Post hoc comparisons for significant effects used paired *t* tests. The analyses were conducted with IBM SPSS v.23 for Windows®.

Changes in the O_2-Hb concentration were defined as the O_2-Hb concentration of aSC or eSC condition subtracted by that of the control condition. Pre-processing of the fNIRS data used the wavelet-minimum description length detrending algorithm method and hemodynamic response function-based low-pass filter for removing artifacts related to cardiac, breathing, and vasomotor changes (Jang et al., 2009). For all participants, the onset vectors were specified manually, and the onset and duration of each block were defined from those registered in each scan. The changes in the O_2-Hb concentration at the participant and group levels were derived using NIRS-SPM (Tak et al., 2011). The group-level changes in O_2-Hb concentration SPM *t* statistic map, with statistical significance set at $p \leq 0.05$. The *t* statistics were used to plot the channel-specific fNIRS as shown in Figure 5

(see Results). Pearson's correlation coefficients of the changes in the O_2-Hb concentration among the channels were computed for the aSC and eSC conditions using the R packages for statistical computing (R Core Team, 2017). Hierarchical clustering method was employed to further group and visualize the patterns of the correlograms available in the R package (Murtagh, 1985).

The least absolute shrinkage and selection operator-regularized principal component (LASSO-PCR) (e.g. Ryali, Chen, Supekar, & Menon, 2012), a machine learning-based regression analysis, was conducted to explore the relationships between the behavioral responses and the brain activities. That is, LASSO-PCR was to predict the participants' RTs from the 44 channel-specific changes in the O_2-Hb concentration. The advantage of LASSO-PRC is that it can minimize the overfitting shortcomings due to the large number of multiple comparisons as used in other statistical methods. The LASSO-PCR model was:

$$\hat{\beta}^{lasso} = min\beta(y - Z\beta)'(y - Z\beta) + \lambda \sum_{J=1}^{p} |\beta j|$$

whereby $\sum_{J=1}^{p}|\beta j|$ is the absolute size of the least square estimate; and Z is the channel-specific change in the O_2-Hb concentration. When Z_j weakly relates with Y, the value of βj would approach zero. To further control within group variability, RT of the control condition was entered as a regressor variable in the regression model. All the LASSO related analyses were conducted with the R packages of statistical computing (Friedman, Hastie, & Tibshirani, 2009).

3. Results

3.1 Behavioral Results

The data of one participant was excluded from the analyses because the corresponding data was discarded from the NIRS-SPM analysis. The Validity × Condition effect on the RTs was statistically significant (F (1, 20) = 10.45, p < .01) (Figure 3). The RTs for the valid trials were significantly faster than those for the invalid trials in both the aSC condition (t (20) = -4.96, p < .001) and eSC conditions (t (20) = -6.71, p < .001). The eSC RTs

were significantly faster than the aSC RTs (t (20) = -3.28, p < .01). The RTs of both conditions were significantly faster than those of the control condition (t (20) = 5.69, p < .001). The differences in the between-condition RTs were not significant for the invalid trials (t (20) = 0.13, p > .05). The accuracy rates were 91.6 ± 2.3% for the eSC condition and 87.3 ± 3.7% for the aSC condition.

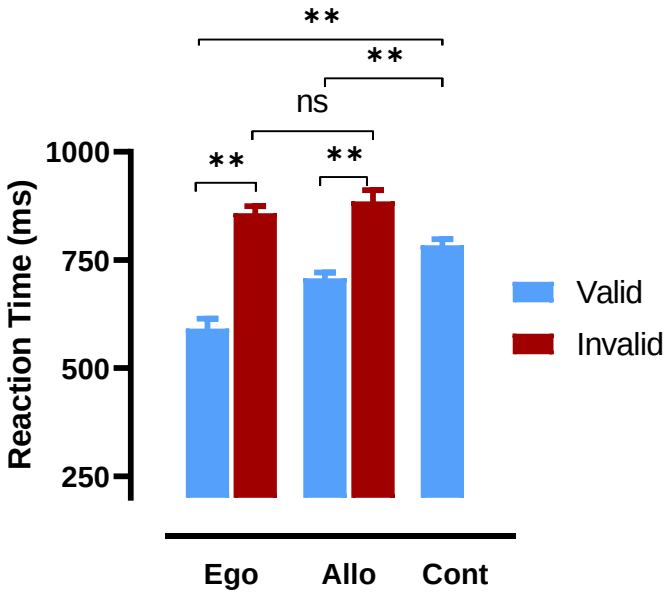

Figure 3. Comparisons of reaction times across the egocentric, allocentric, and control conditions. Note: Error bars are standard errors. ** = p < .001.

3.2 fNIRS Results

The NIRS-SPM-based contrast analysis included 21 participants as the data of one participant had error during signal recording. No significant clusters of activation were revealed in the eSC > aSC contrast, and vice versa. Significant changes in O_2-Hb concentration were found for the aSC > Control contrast in a large right cluster of activation including the right post-central gyrus (Ch. 16) (t (20) = 3 (maxima), p < .05), IPS (Ch. 12) (t (20) = 3 (maxima), p < .05), IPL (Ch. 20) (t (20) = 3 (maxima), p < .05), and TPJ (Ch. 21) (t (20) = 3 (maxima), p < .05), and a small left cluster in the IPL (Ch.20) (t(20) = 3 (maxima), p <.05) (Figure 4). Significant clusters of activation found in the eSC > Control contrast were

in the right post-central gyrus (Ch. 16) (t (20) = 2.6 (maxima), p < .05) and IPL (t (20) = 2.6 (maxima), p < .05).

Channel-specific fNIRS t values plotted on an MNI-compatible canonical brain show that the left hemisphere had lower t values (i.e. cortical activities) than the right hemisphere in both the spatial coding conditions (t (20) = 1.83 - 2.20, p = .05) (Figure 5).

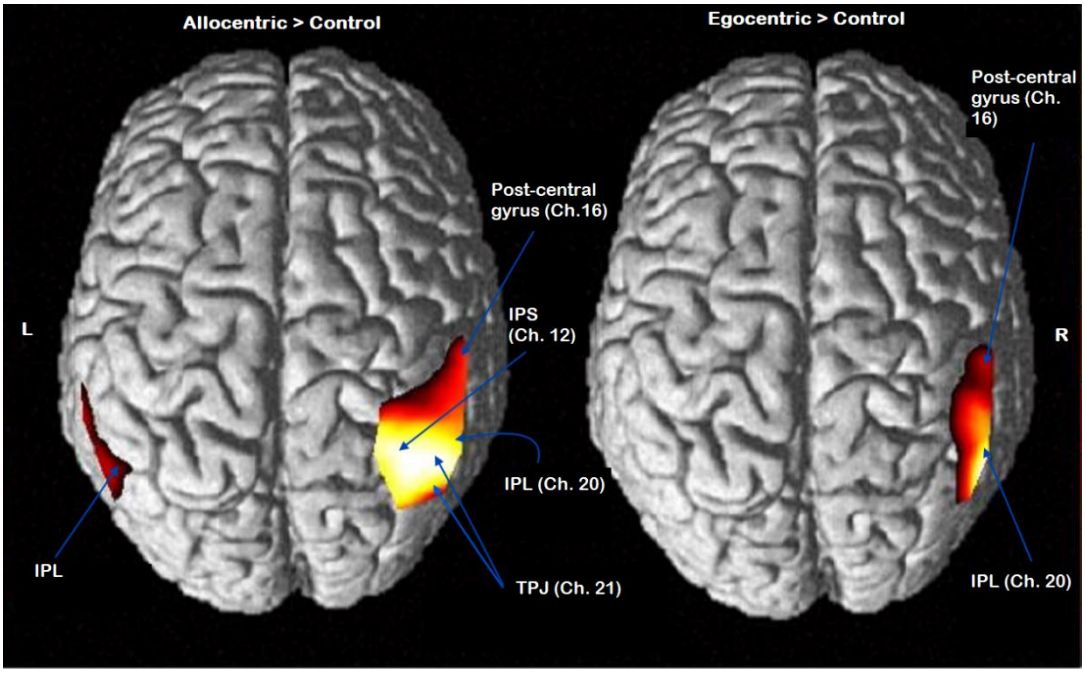

Figure 4. Significant cortical activities in the right and left hemispheres for the aSC > Control and eSC > Control contrasts. The group mean t-values on O_2-Hb were superimposed onto the T1 template mapped on the MNI coordinate values. Note: The channel numbers shown correspond to those in Figure 2.

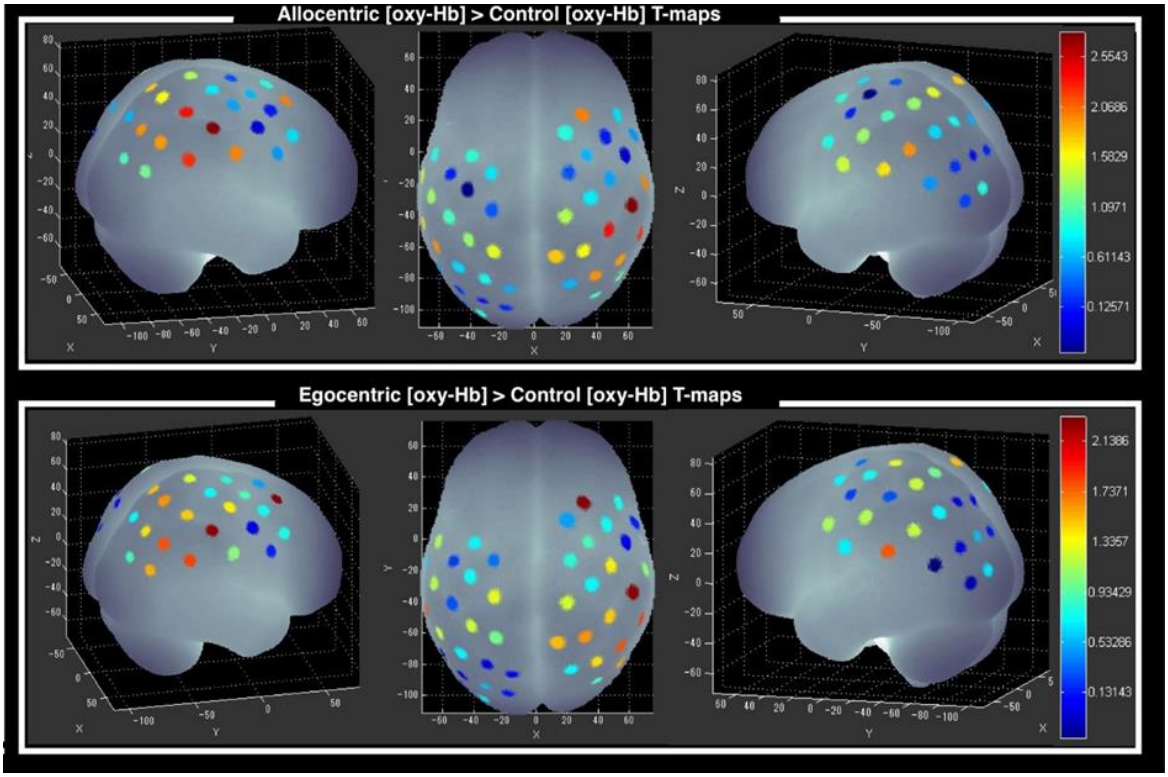

Figure 5. Channel-specific fNIRS plot on the right and left hemispheres for both the allocentric and egocentric conditions. Note: t-values are group-based O_2-Hb mapped on the channels 1 to 44 for allocentric > control and egocentric > control comparisons.

Correlations of the aSC minus Control or eSC minus Control O_2-Hb concentration changes among the channels were explored. In the aSC condition, in the right hemisphere, there were significant positive correlations between the channels in the right frontal region (channels 2, 10, 14) and those in the right parietal region at the right SPL (channels 12, 16) ($p < .01$; Figure 6). Significant negative correlations were observed between a cluster of channels in the right frontal regions at MFG (channels 10 and 14) and SFG (channels 1, 2) and those in the right parietal region (channels 9, 13, and 21) ($p < .01$). In the left hemisphere, similar positive correlations were revealed between a cluster of channels in the left precentral gyrus (channels 27, 36, 37 and 41) and the left parietal regions at the SPL (channels 38, 43, and 44) and the IPL (channels 24, 29, 39(($p < .001$ to .01). Another clusters of channel correlations were between the left SFG (channel 41) and the left parietal region (channel 24 and 29 ($p < 0.001$). In the eSC condition, no negative correlations were revealed. In the right hemisphere, the significant frontal to parietal

channel correlations were only found between the frontal region (channels 2, 10, 14) and the SPL (channels 12, 16 ($p < .01$; Figure 7). In the left hemisphere, the frontal to parietal correlations were between the precentral gyrus (channels 27, 36, 37 and 41) and the SPL (channels 38, 43, and 44; $p < .01$) and IPL (channels 24, 29, 39; $p < .001$); and between the SFG (channel 41) and the parietal region (channels 24 and 29; LH: $p < 0.001$).

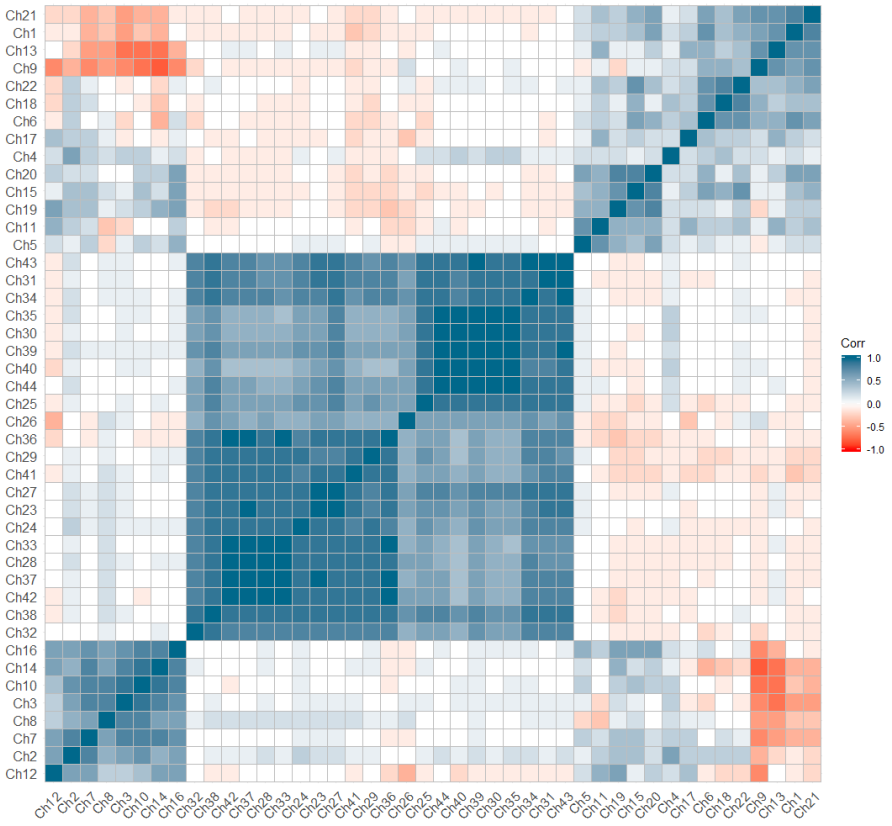

Figure 6. Correlational matrix of channel-specific change in O_2-Hb concentration of Allocentric minus Control condition. Hierarchical clustering is used to group the correlation coefficients.

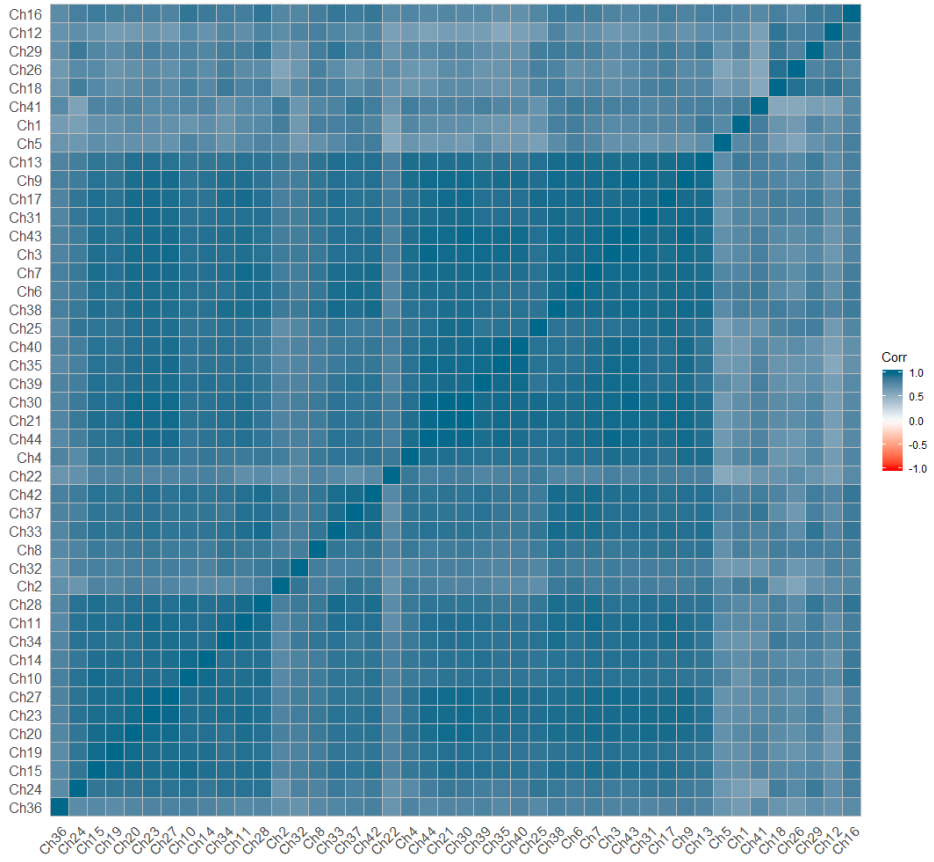

Figure 7. Correlational matrix of channel-specific change in O_2-Hb concentration of Egocentric minus Control condition. Hierarchical clustering is used to group the correlation coefficients.

3.3 LASSO-PCR Regression

The regression model built for the aSC condition included six channels, which explained 59.5% of the total variance (Table 1a). Among them, the changes in the O_2-Hb concentration in two channels significant predicted the RTs. They were channel 2 corresponded to the right SFG F (6, 17) = 6.63, p = 0.04, and channel 27 corresponded to the left precentral gyrus (PG) F (6, 17) = 6.63, p = 0.038. In contrast, the model built for the eSC condition included eight channels, which explained 54.1% of the total variance (Table 1b). Among them, all the three significant channels predicting the RTs were in the right hemisphere: channel 1 F (8, 15 = 4.38, p = .029 and channel 5 F (8, 15) = 4.38, p = .002, corresponded to the right SFG, while channel 22 F (8, 15) = 4.38, p < .001, corresponded to the caudal part of right IPL and the right middle temporal gyrus (MTG).

Table 1

Summary of LASSO-PRC regression of changes in O_2-Hb concentration in fNIRS channels predicting RTs in allocentric and egocentric conditions.

	Estimate	Std. Error	t-value	*p*-value	MNI Coordinates	Anatomical Labelling
a. Allocentric SC						
Ch.26	-38.00	43.51	-0.87	.394	-44, -91, 5	MOG (L)
Ch.27	-242.90	108.45	-2.24	.038*	-60, -2, 41	PG (L)
Ch.02	281.97	126.77	2.22	.040*	21, -13, 76	SFG (R)
Ch.04	179.01	96.27	1.86	.080	14, -64, 71	SPL (R)
Ch.05	-62.25	41.38	-1.50	.150	30, 22, 62	SFG (R)
Ch.06	-76.29	147.18	-0.52	.610	32, -2, 68	SFG (R)
b. Egocentric SC						
Ch.26	-98.84	108.02	-0.92	.374	-44, -91, 5	MOG (L)
Ch.31	-39.14	172.14	-0.23	.823	-32, -99, 11	MOG (L)
Ch.36	-231.55	127.13	-1.82	.088	-38, -3, 65	PG (L)
Ch.01	-327.73	136.33	-2.40	.029*	20, 12, 71	SFG (R)
Ch.05	770.58	215.26	3.58	.002*	30, 22, 62	SFG (R)
Ch.14	-161.74	229.72	-0.70	.492	51, 23, 44	MFG (R)
Ch.15	-127.62	235.01	-0.54	.595	56, -2, 53	PoG (R)
Ch.22	477.39	111.12	4.29	<.001	52, -76, 26	pIPL (R)

Note. *p<.05. MNI=Montreal Neurological Institute. MOG = middle occipital gyrus. PG = precentral gyrus. SFG = superior frontal gyrus. MFG = middle frontal gyrus. pIPL = posterior inferior parietal lobule. SPL = superior parietal lobule. PoG = postcentral gyrus.

4. General Discussion

The custom-designed cue-to-target paradigm revealed different patterns of cortical activities for allocentric and egocentric spatial coding. First, the predictive model based on the changes in the O_2-Hb concentration suggested that cortical activities in the right SFG. The cortical activities in the bilateral IPL, including the PoG, were also found to be common to both types of spatial coding, but it was bilateral activities for allocentric compared to only the right hemispheric activities for the egocentric condition. They suggested possible top-down attention shift and maintenance (i.e. IPL) and response mapping (i.e. SFG) occurred in both types of spatial coding. The common cortical activities revealed supported the first hypothesis set for this study that both aSC and eSC would involve dorsal attention network. Cortical activities found unique to allocentric spatial coding were in the left IPL, the right TPJ, right IPS, and left PG for allocentric, which were not observed in egocentric spatial coding. These results suggested plausible involvements of additional visuospatial memory and updating (i.e. precuneus) (Wolbers, Hegarty, Büchel, & Loomis, 2008) and maintaining object-directed actions (i.e. IPS) (to maintain object-directed actions; James, Humphrey, Gati, Menon, & Goodale, 2002).

The cue-target paradigm used in this study involved orienting attention and attention control. The behavioral results showed that the allocentric spatial coding had longer RTs than the egocentric spatial coding. As egocentric spatial coding is location based, the longer RTs suggest that the position-based processing involved in the allocentric spatial coding might have involved additional steps in the cue-to-target process. Our results are comparable to previous studies in which the tasks had an orienting component in the cue phase (Au, 2014; Barrett et al., 2001). However, the results are different from two other studies which embedded similar cognitive processes but found no significant between-condition differences in RTs (see e.g.: Committeri et al., 2004; Kozhevnikov, Motes, Rasch, & Blajenkova, 2006). The inconsistent results perhaps are due to the difference in the task rules that, in Committeri et al. (2004) and Kozhevnikov et al. (2006), the navigation of spatial locations was based on the fixed target mapping rules set at the beginning of the task condition compared with the time-locked trial-by-trial rule informed by the cue in this study.

The activities in the SFG was revealed to be the strongest predictor of the subjects' task performances in both the allocentric and egocentric conditions. In the montage, the SFG corresponds to the posterior subregion of SFG (SFGp), which mediates motor control in sensorimotor-related tasks (Li et al., 2013). Besides, the SFG involves control attention pertinent to location when the cue was time locked to the anticipation of the upcoming target stimuli (Corbetta & Shulman, 2002; Hopfinger, Buonocore, & Mangun, 2000). The activities in the SFG suggested that attention control and stimulus-response mapping processes are the common neural processes to both types of spatial coding. The other regions involved in both types were the IPL and PoG which were reported to be parts of the "task positive network" (Fox et al., 2005). Together with SFG, IPL was found relating to attention control of cue stimuli (Noudoost, Chang, Steinmetz, & Moore, 2010). The PoG which includes SMA, SEF and pre-SMA mediates vigilance for visually guided task-switching (Nachev, Kennard, & Husain, 2008) and responses to target stimuli (Ptak, 2012). Our findings further reinforce those reported in previous studies that in both spatial coding types the task-taking processes involve stimulus-response mapping and responses to target stimuli in addition to attention control (e.g. Fink et al., 2003; Liu et al., 2017; Neggers et al., 2006; Saj et al., 2014).

The main differences revealed between the two types of spatial coding are in the results of the right TPJ and left PG. The fNIRS results showed significant cortical activities in the TPJ, alongside with the IPS and PG, only in the allocentric but not in egocentric condition. The TPJ has been reported to play a major role in mediating reorienting attention (Corbetta, Kincade, Lewis, Snyder, & Sapir, 2005; Krall et al., 2015). Our results further suggested that allocentric, when compared with egocentric spatial coding, would have demanded more reorienting attention when encoding the spatial relationships among the objects. In this study, when engaging in the allocentric trial, the subjects were required to identify the distractor-target triad of which the locations were at least a 45° angular distance from the cued location. The participant would have to reorientate his or her attention to capture the new positions of the distractor-target triad before making a response. The significant results obtained for the cortical activities in the caudal parts of IPL (aka angular gyrus) (channels 17, 21 and 22) offered support to our proposition that reorienting attention process is unique to allocentric spatial coding. Angular gyrus, as part

of the task negative network (Fox et al., 2005), has been found to mediate manipulation of mental representation and reorient attention to relevant information.

The main discrepancies between the results of our study and those of Szczepanski et al. (2013) are in the latter not revealing the involvements of TPJ and SPL in the allocentric condition and IPL in the egocentric condition. For TPJ and IPL, our results are consistent with those of a previous study (review: Kravitz, Saleem, Baker, & Mishkin, 2011), suggesting updating visuospatial information would have been a process in both spatial coding conditions. For SPL, the result indicated maintaining working memory during top-down processing (Corbetta & Shulman, 2002) may be unique to allocentric but not egocentric spatial coding. Nevertheless, the discrepancies in the results with Szczepanski et al. (2013) may have been due to the difference in the task design between the two studies. Future study is call for verifying this speculation.

This study has several limitations and readers are reminded to interpret the results with caution. First, the experimental task used was relatively more complex than the tasks employed in other spatial coding studies, particularly in the identification of the target among the distractors. Generalization of the results would need to consider the task-specific differences. Second, the NIRS method tends to capture cortical activities occurred superficially to the cortex (2–3 cm below the scalp)(Toronov et al., 2001), activities emitted from deeper neural structures such as those from MTL could have been excluded in this study. Third, due to the limited coverage by the fNIRS probe montage adopted in this study, activities apart from those emitting from the dorsal aspect of the scalp might have been missed such as middle temporal cortex. Last but not least is the use of the block design for grouping the same spatial coding trials which could have inflated the biases due to the adoption of task-taking strategies among the participants. Future study is to test the robustness of the results by using similar test design but varying the task difficulty level. Other methods of brain imaging such as functional magnetic resonance imaging and of event-related design for exploring the possible involvement of other brain structures in spatial coding.

To conclude, this study's results revealed similarities and differences between the allocentric and egocentric spatial coding processes. The similarities rest with the cortical activities in the SFG and IPL, including PG, suggesting both types of spatial coding involve

attention control and stimulus-response mapping. The dissociation between the two types of spatial coding is in the cortical activities in the left IPL, IPS, and the right TPJ suggesting reorienting of attention and visual working memory are involved in allocentric but not egocentric spatial coding. The findings offer plausible explanation to the observations that individuals showed difficulties in performing allocentric spatial coding but not egocentric spatial coding. Older individuals with neurodegeneration(Colombo et al., 2017; Lithfous, Dufour, Blanc, & Després, 2014) have been reported to present with decline performances in allocentric but not egocentric spatial coding tasks. It is plausible that the cognitive processes unique to allocentric spatial coding could have been compromised by the insults to the brain in both cases. Future studies is to test the robustness of the uniqueness of allocentric and egocentric spatial coding by employing visuospatial tasks of different designs. Studies involving post-stroke patients with specific brain lesions can be conducted to inform the application of spatial coding tests in clinical practices

Acknowledgement

The General Research Fund of Research Grant Council of Hong Kong (151044) partially supported this study. The authors thank the University Research Facility in Behavioral and Systems Neuroscience, The Hong Kong Polytechnic University, for its support.

References

Au, B. K. (2014). *Aging effect on egocentric and allocentric frames of reference in visual attention: an event-related potential (ERP) study*. (PhD dissertation). The Hong Kong Polytechnic University, Hong Kong.

Barrett, D. J., Bradshaw, M. F., Rose, D., Everatt, J., & Simpson, P. J. (2001). Reflexive shifts of covert attention operate in an egocentric coordinate frame. *Perception, 30*(9), 1083-1091.

Burgess, N. (2006). Spatial memory: how egocentric and allocentric combine. *Trends Cogn. Sci., 10*(12), 551-557. doi:10.1016/j.tics.2006.10.005

Burgess, N. (2008). Spatial cognition and the brain. *Ann. N. Y. Acad. Sci., 1124*(1), 77-97. doi:10.1196/annals.1440.002

Castiello, U. (2005). The neuroscience of grasping. *Nat. Rev. Neurosci., 6*(9), 726-736. doi:10.1038/nrn1744

Chen, Q., Weidner, R., Weiss, P. H., Marshall, J. C., & Fink, G. R. (2012). Neural interaction between spatial domain and spatial reference frame in parietal-occipital junction. *J. Cogn. Neurosci., 24*(11), 2223-2236. doi:10.1162/jocn_a_00260

Chun, M. M., Golomb, J. D., & Turk-Browne, N. B. (2011). A taxonomy of external and internal attention. *Annu. Rev. Psychol., 62*, 73-101. doi:10.1146/annurev.psych.093008.100427

Colombo, D., Serino, S., Tuena, C., Pedroli, E., Dakanalis, A., Cipresso, P., & Riva, G. (2017). Egocentric and allocentric spatial reference frames in aging: A systematic review. *Neuroscience & Biobehavioral Reviews, 80*, 605-621. doi:https://doi.org/10.1016/j.neubiorev.2017.07.012

Committeri, G., Galati, G., Paradis, A. L., Pizzamiglio, L., Berthoz, A., & LeBihan, D. (2004). Reference frames for spatial cognition: different brain areas are involved in viewer-, object-, and landmark-centered judgments about object location. *J Cognitive Neurosci, 16*(9), 1517-1535. doi:10.1162/0898929042568550

Cooper, A. C. G., & Humphreys, G. W. (2000). Coding space within but not between objects: evidence from Balint's syndrome. *Neuropsychologia, 38*(6), 723-733. doi:10.1016/s0028-3932(99)00150-5

Cope, M., & Delpy, D. T. (1988). System for long-term measurement of cerebral blood and tissue oxygenation on newborn infants by near infra-red transillumination. *Med. Biol. Eng. Comput., 26*(3), 289-294. doi:10.1007/BF02447083

Corbetta, M., Kincade, M. J., Lewis, C., Snyder, A. Z., & Sapir, A. (2005). Neural basis and recovery of spatial attention deficits in spatial neglect. *Nat. Neurosci., 8*(11), 1603-1610. doi:10.1038/nn1574

Corbetta, M., & Shulman, G. L. (2002). Control of goal-directed and stimulus-driven attention in the brain. *Nat. Rev. Neurosci., 3*(3), 201-215. doi:10.1038/nrn755

Culham, J. C., & Valyear, K. F. (2006). Human parietal cortex in action. *Curr. Opin. Neurobiol., 16*(2), 205-212. doi:10.1016/j.conb.2006.03.005

Dean, H. L., & Platt, M. L. (2006). Allocentric spatial referencing of neuronal activity in macaque posterior cingulate cortex. *Journal of Neuroscience, 26*(4), 1117-1127.

Desimone, R., & Duncan, J. (1995). Neural mechanisms of selective visual attention. *Annu. Rev. Neurosci., 18*(1), 193-222. doi:10.1146/annurev.ne.18.030195.001205

Eickhoff, S. B., Stephan, K. E., Mohlberg, H., Grefkes, C., Fink, G. R., Amunts, K., & Zilles, K. (2005). A new SPM toolbox for combining probabilistic cytoarchitectonic maps and functional imaging data. *Neuroimage, 25*(4), 1325-1335. doi:10.1016/j.neuroimage.2004.12.034

Ekstrom, A. D., Arnold, A. E., & Iaria, G. (2014). A critical review of the allocentric spatial representation and its neural underpinnings: toward a network-based perspective. *Front. Hum. Neurosci., 8*, 803. doi:10.3389/fnhum.2014.00803

Epstein, R. A. (2008). Parahippocampal and retrosplenial contributions to human spatial navigation. *Trends Cogn. Sci., 12*(10), 388-396. doi:10.1016/j.tics.2008.07.004

Filimon, F. (2015). Are All Spatial Reference Frames Egocentric? Reinterpreting Evidence for Allocentric, Object-Centered, or World-Centered Reference Frames. *Front. Hum. Neurosci., 9*, 648. doi:10.3389/fnhum.2015.00648

Fink, G. R., Marshall, J. C., Weiss, P. H., Stephan, T., Grefkes, C., Shah, N. J., . . . Dieterich, M. (2003). Performing allocentric visuospatial judgments with induced distortion of the egocentric reference frame: an fMRI study with clinical implications. *Neuroimage, 20*(3), 1505-1517.

Fox, M. D., Corbetta, M., Snyder, A. Z., Vincent, J. L., & Raichle, M. E. (2006). Spontaneous neuronal activity distinguishes human dorsal and ventral attention systems. *Proc. Natl. Acad. Sci. U. S. A., 103*(26), 10046-10051. doi:10.1073/pnas.0604187103

Fox, M. D., Snyder, A. Z., Vincent, J. L., Corbetta, M., Van Essen, D. C., & Raichle, M. E. (2005). The human brain is intrinsically organized into dynamic, anticorrelated functional networks. *Proc. Natl. Acad. Sci. U. S. A., 102*(27), 9673-9678. doi:10.1073/pnas.0504136102

Friedman, J., Hastie, T., & Tibshirani, R. (2009). glmnet: Lasso and elastic-net regularized generalized linear models. *R package version, 1*(4).

Galati, G., Committeri, G., Sanes, J. N., & Pizzamiglio, L. (2001). Spatial coding of visual and somatic sensory information in body-centred coordinates. *Eur. J. Neurosci., 14*(4), 737-746.

Galati, G., Lobel, E., Vallar, G., Berthoz, A., Pizzamiglio, L., & Le Bihan, D. (2000). The neural basis of egocentric and allocentric coding of space in humans: a functional magnetic resonance study. *Exp. Brain Res., 133*(2), 156-164.

Gomez, A., Cerles, M., Rousset, S., Remy, C., & Baciu, M. (2014). Differential hippocampal and retrosplenial involvement in egocentric-updating, rotation, and allocentric processing during online spatial encoding: an fMRI study. *Front. Hum. Neurosci., 8*, 150. doi:10.3389/fnhum.2014.00150

Heinzel, S., Haeussinger, F. B., Hahn, T., Ehlis, A. C., Plichta, M. M., & Fallgatter, A. J. (2013). Variability of (functional) hemodynamics as measured with simultaneous fNIRS and fMRI during intertemporal choice. *Neuroimage, 71*, 125-134. doi:10.1016/j.neuroimage.2012.12.074

Hopfinger, J. B., Buonocore, M. H., & Mangun, G. R. (2000). The neural mechanisms of top-down attentional control. *Nat. Neurosci., 3*(3), 284-291. doi:10.1038/72999

Iaria, G., Chen, J. K., Guariglia, C., Ptito, A., & Petrides, M. (2007). Retrosplenial and hippocampal brain regions in human navigation: complementary functional contributions to the formation and use of cognitive maps. *Eur. J. Neurosci., 25*(3), 890-899. doi:10.1111/j.1460-9568.2007.05371.x

James, T. W., Humphrey, G. K., Gati, J. S., Menon, R. S., & Goodale, M. A. (2002). Differential effects of viewpoint on object-driven activation in dorsal and ventral streams. *Neuron, 35*(4), 793-801.

Jang, K. E., Tak, S., Jung, J., Jang, J., Jeong, Y., & Ye, J. C. (2009). Wavelet minimum description length detrending for near-infrared spectroscopy. *J. Biomed. Opt., 14*(3), 034004. doi:10.1117/1.3127204

Kocsis, L., Herman, P., & Eke, A. (2006). The modified Beer–Lambert law revisited. *Phys. Med. Biol., 51*(5), N91. doi:10.1088/0031-9155/51/5/N02

Kozhevnikov, M., Motes, M. A., Rasch, B., & Blajenkova, O. (2006). Perspective-taking vs. mental rotation transformations and how they predict spatial navigation performance. *Applied Cognitive Psychology, 20*(3), 397-417.

Krall, S., Rottschy, C., Oberwelland, E., Bzdok, D., Fox, P., Eickhoff, S., . . . Konrad, K. (2015). The role of the right temporoparietal junction in attention and social interaction as revealed by ALE meta-analysis. *Brain Structure and Function, 220*(2), 587-604. doi:10.1007/s00429-014-0803-z

Kravitz, D. J., Saleem, K. S., Baker, C. I., & Mishkin, M. (2011). A new neural framework for visuospatial processing. *Nat. Rev. Neurosci., 12*(4), 217-230. doi:10.1038/nrn3008

Lithfous, S., Dufour, A., Blanc, F., & Després, O. (2014). Allocentric but not egocentric orientation is impaired during normal aging: An ERP study. *Neuropsychology*, *28*(5), 761.

Liu, N., Li, H., Su, W., & Chen, Q. (2017). Common and specific neural correlates underlying the spatial congruency effect induced by the egocentric and allocentric reference frame. *Hum. Brain Mapp.*, *38*(4), 2112-2127. doi:10.1002/hbm.23508

Milner, A. D., & Goodale, M. A. (2008). Two visual systems re-viewed. *Neuropsychologia, 46*(3), 774-785. doi:10.1016/j.neuropsychologia.2007.10.005

Murtagh, F. (1985). Multidimensional clustering algorithms. In *Compstat Lectures, Vienna: Physika Verlag, 1985*.

Nachev, P., Kennard, C., & Husain, M. (2008). Functional role of the supplementary and pre-supplementary motor areas. *Nature Reviews Neuroscience, 9*, 856. doi:10.1038/nrn2478

Neggers, S. F., Van der Lubbe, R. H., Ramsey, N. F., & Postma, A. (2006). Interactions between ego- and allocentric neuronal representations of space. *Neuroimage, 31*(1), 320-331. doi:10.1016/j.neuroimage.2005.12.028

Noudoost, B., Chang, M. H., Steinmetz, N. A., & Moore, T. (2010). Top-down control of visual attention. *Curr. Opin. Neurobiol.*, *20*(2), 183-190. doi:10.1016/j.conb.2010.02.003

Posner, M. I. (1980). Orienting of attention. *Q J Exp Psychol, 32*(1), 3-25. doi:10.1080/00335558008248231

Ptak, R. (2012). The frontoparietal attention network of the human brain: action, saliency, and a priority map of the environment. *Neuroscientist, 18*(5), 502-515. doi:10.1177/1073858411409051

R Core Team. (2017). R: A language and environment for statistical computing.

Ryali, S., Chen, T., Supekar, K., & Menon, V. (2012). Estimation of functional connectivity in fMRI data using stability selection-based sparse partial correlation with elastic net penalty. *Neuroimage, 59*(4), 3852-3861. doi:10.1016/j.neuroimage.2011.11.054

Saj, A., Cojan, Y., Musel, B., Honore, J., Borel, L., & Vuilleumier, P. (2014). Functional neuro-anatomy of egocentric versus allocentric space representation. *Neurophysiol. Clin.*, *44*(1), 33-40. doi:10.1016/j.neucli.2013.10.135

Singh, A. K., Okamoto, M., Dan, H., Jurcak, V., & Dan, I. (2005). Spatial registration of multichannel multi-subject fNIRS data to MNI space without MRI. *Neuroimage, 27*(4), 842-851. doi:10.1016/j.neuroimage.2005.05.019

Szczepanski, S. M., Pinsk, M. A., Douglas, M. M., Kastner, S., & Saalmann, Y. B. (2013). Functional and structural architecture of the human dorsal frontoparietal attention network. *Proc Natl Acad Sci U S A, 110*(39), 15806-15811. doi:10.1073/pnas.1313903110

Tak, S., Yoon, S. J., Jang, J., Yoo, K., Jeong, Y., & Ye, J. C. (2011). Quantitative analysis of hemodynamic and metabolic changes in subcortical vascular dementia using simultaneous near-infrared spectroscopy and fMRI measurements. *Neuroimage, 55*(1), 176-184. doi:10.1016/j.neuroimage.2010.11.046

Toronov, V., Webb, A., Choi, J. H., Wolf, M., Michalos, A., Gratton, E., & Hueber, D. (2001). Investigation of human brain hemodynamics by simultaneous near-infrared spectroscopy and functional magnetic resonance imaging. *Med. Phys., 28*(4), 521-527. doi:10.1118/1.1354627

Vossel, S., Geng, J. J., & Fink, G. R. (2014). Dorsal and ventral attention systems: distinct neural circuits but collaborative roles. *Neuroscientist, 20*(2), 150-159. doi:10.1177/1073858413494269

Wolbers, T., Hegarty, M., Büchel, C., & Loomis, J. M. (2008). Spatial updating: how the brain keeps track of changing object locations during observer motion. *Nature neuroscience, 11*(10), 1223.

Zaehle, T., Jordan, K., Wustenberg, T., Baudewig, J., Dechent, P., & Mast, F. W. (2007). The neural basis of the egocentric and allocentric spatial frame of reference. *Brain Res, 1137*(1), 92-103. doi:10.1016/j.brainres.2006.12.044

Zhang, H., & Ekstrom, A. (2013). Human neural systems underlying rigid and flexible forms of allocentric spatial representation. *Hum. Brain Mapp., 34*(5), 1070-1087. doi:10.1002/hbm.21494